WATER RESOURCES RESEARCH, VOL. 47, W00G10, doi:10.1029/2010WR010333, 2011

An investigation into changes in climate characteristics causing the recent very low runoff in the southern Murray-Darling Basin using rainfall-runoff models

N. J. Potter[1] and F. H. S. Chiew[1]

Received 19 December 2010; revised 11 June 2011; accepted 2 September 2011; published 18 October 2011.

[1] The recent drought in the southern Murray-Darling Basin has seen a larger reduction in annual runoff in many places compared to historical droughts with similar annual rainfall reductions. Several reasons have been suggested for this, including proportionally less autumn and winter rainfall, fewer high rainfall years, and increased temperatures. Using the SIMHYD daily rainfall-runoff model and scenarios of rainfall and potential evapotranspiration, we investigate the causes of the observed runoff reduction over 1997–2008 in the Campaspe river basin, an area representative of the southern Murray-Darling Basin. This method accounts for 83% of the runoff reduction, with the reduction in annual rainfall accounting for 52%. The remainder is not explained by any single hydroclimatic feature but is mostly accounted for by the combination of changes in rainfall variability outside monthly and annual time scales (15%), changed seasonality of rainfall (11%), and increased potential evapotranspiration (5%).

Citation: Potter, N. J., and F. H. S. Chiew (2011), An investigation into changes in climate characteristics causing the recent very low runoff in the southern Murray-Darling Basin using rainfall-runoff models, *Water Resour. Res.*, *47*, W00G10, doi:10.1029/2010WR010333.

1. Introduction

[2] The Murray-Darling Basin (MDB) has recently experienced a prolonged drought for 10–15 years. Particularly in the southern parts of the MDB, mean annual rainfall over the drought period was 10%–20% below the long-term mean in most places, which is the lowest or close to the lowest in more than 100 years of instrumental records [*Potter et al.*, 2010]. The recent drought has often been compared to historical droughts in the MDB, and particularly the World War II drought, which in terms of broad-scale rainfall declines over 10–15 year periods is approximately equal in severity to the recent drought [*Murphy and Timbal*, 2008; *Timbal*, 2009; *Verdon-Kidd and Kiem*, 2009; *Timbal et al.*, 2010]. However, the decline in mean annual runoff in some parts of the southern MDB of over 50% during the recent drought has been much more severe and unprecedented in historical records [*Verdon-Kidd and Kiem*, 2009; *Potter et al.*, 2008, 2010]. Most studies define the start of the drought in the MDB as 1997 [*Chiew et al.*, 2009a], although *Kiem and Verdon-Kidd* [2010] have the dry sequence starting around 1994 in some places. In this study, we define the drought as beginning in 1997 and consider climate and runoff data from 1997 to 2008. The Campaspe river basin (see Figure 1) was chosen as a representative area of the southern MDB as the annual rainfall and runoff reductions over the recent drought in the Campaspe were typical of the largest reductions in modeled runoff in the southern MDB. The Campaspe river basin has an area of nearly 4000 km^2, with the dominant land use dryland agriculture. More information is provided by the *Commonwealth Scientific and Industrial Research Organisation* (*CSIRO*) [2008a]. Figure 2 shows annual rainfall and runoff in the Campaspe river basin from 1895 to 2008.

1.1. Runoff Reductions in the Southern MDB During the Recent Drought

[3] The recent reductions in annual runoff over in the southern MDB can be considered more severe than the corresponding reductions in annual rainfall. The average relative magnitude of annual runoff anomalies to annual rainfall anomalies is generally measured using elasticities [e.g., *Schaake*, 1990; *Sankarasubramanian et al.*, 2001]. The rainfall elasticity of runoff of a catchment is the average ratio of a percentage change in annual runoff to a percentage change in annual rainfall. There are many ways to define this elasticity, which differ primarily in the assumptions underlying the relationship between annual rainfall and runoff. Model-based approaches to estimating the rainfall elasticity of runoff include derivations from semiempirical theory [e.g., *Dooge et al.*, 1999; *Koster and Suarez*, 1999; *Milly and Dunne*, 2002; *Potter and Zhang*, 2009] and simulations from process-based models [*Chiew*, 2006]. Data-based approaches to estimating elasticity include regression models and surface fitting procedures [e.g., *Vogel et al.*, 1999; *Fu et al.*, 2007] and nonparametric estimators [*Sankarasubramanian et al.*, 2001]. *Sankarasubramanian et al.* [2001] reviewed a number of approaches and recommended using a median-based approach, which does not require any particular model assumptions. *Chiew* [2006] calculated elasticity of streamflow for a number of catchments

[1]CSIRO Water for a Healthy Country National Research Flagship, CSIRO Land and Water, Canberra, ACT, Australia.

0043-1397/11/2010WR010333

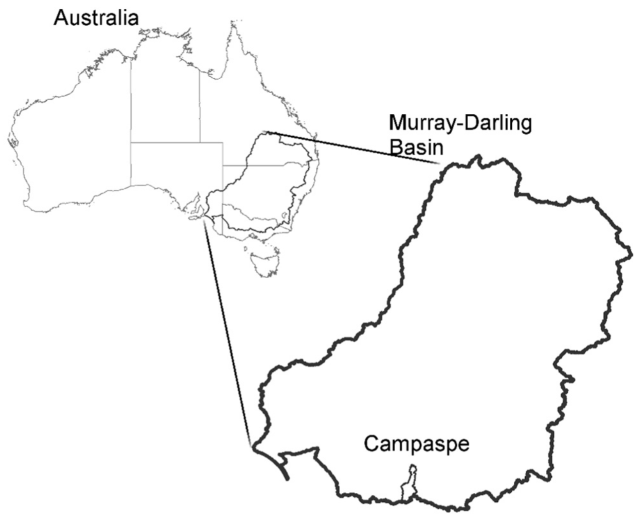

Figure 1. Location of the Campaspe river basin within the Murray-Darling Basin.

in Australia. The median-based estimates in southeast Australia are generally between 2 and 3.5, indicating that a 10% reduction in annual rainfall will tend to result in a 20%–35% reduction in annual runoff. In the Campaspe river basin over 1997–2008, mean annual rainfall decreased by 15%, whereas runoff decreased by 59% (Table 1). The rainfall elasticity of runoff in the Campaspe calculated using the median-based estimate is 2.6. This suggests that on the basis of the historical data a reduction in mean annual rainfall of 15% should lead, on average, to a reduction in mean annual runoff of only 39%. In this study we explore the reasons for this larger than expected reduction in runoff over 1997–2008. The attribution of particular instances of low runoff cannot be assessed using elasticities or sensitivity relationships as these methods are based on long-term average conditions. These

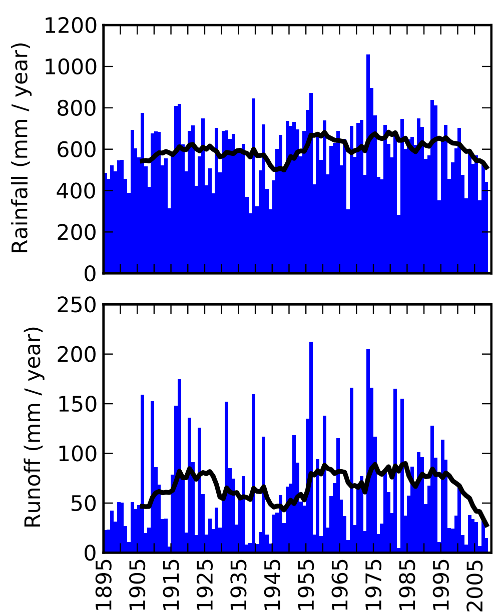

Figure 2. Annual rainfall and runoff in the Campaspe river basin over the entire study period (1895–2008).

Table 1. Mean Annual Rainfall, Potential Evapotranspiration (PET), and Runoff in the Campaspe River Basin

	Rainfall	PET	Runoff
Annual mean over 1895–1996 (mm yr^{-1})	602	1185	68.0
Annual mean over 1997–2008 (mm yr^{-1})	513	1213	28.1
Percentage difference between 1997–2008 and 1895–1996	−15%	2.4%	−59%
Trend over 1950–2008 (mm decade^{-1})	−24	8.8	−9.0

approaches can only tell us that mean annual runoff in the southern MDB during the recent drought has been much lower compared to mean annual runoff in previous droughts with similar reductions in mean annual rainfall.

[4] The relative severity of the runoff decrease can also be analyzed in terms of the average recurrence interval of recent rainfall and runoff, which can be interpreted as the expected waiting time for an equally severe multiyear annual rainfall or runoff reduction under the assumption of stationary climate [*Potter et al.*, 2010]. The average recurrence interval for the reduction in mean annual rainfall over most of the southern MDB during 1997–2006 was estimated at 20–50 years. However, the estimated average recurrence interval for the corresponding reduction in mean annual runoff was considerably larger in the southern MDB during 1997–2006, exceeding 300 years in the southernmost part of the MDB [*Potter et al.*, 2010]. If the reduction in annual runoff had been similar in magnitude to the reduction expected on the basis of similar annual rainfall reductions in the historical record, the average recurrence intervals for recent rainfall and runoff would have been similar. So, although the reductions in rainfall over the past 10–15 years are similar to comparatively severe droughts during the twentieth century, the corresponding reduction in runoff has been much more severe compared to those historical droughts.

1.2. Causes of Lower Runoff

[5] Several reasons have been suggested for the greater reduction in annual runoff in the southern MDB compared to historical droughts with similar low mean annual rainfall [*Nicholls*, 2004; *Murphy and Timbal*, 2008; *Cai and Cowan*, 2008b; *Kiem and Verdon-Kidd*, 2010; *Verdon-Kidd and Kiem*, 2009; *National Climate Centre*, 2010; *Potter et al.*, 2010; *Timbal et al.*, 2010]. These include (1) the greater proportional reduction in autumn and winter rainfall in the recent drought, which had a larger effect on the runoff in the southern MDB, where most runoff occurs in the winter months, (2) the observed increase in annually averaged daily mean and maximum temperatures in the southern MDB since 1950, which may accentuate the reduction in runoff caused by reductions in rainfall, (3) a lack of high rainfall years, and (4) changes in the daily distribution of rainfall amounts and rainfall sequencing. We briefly review each of these below.

[6] Rainfall in southeast Australia has been associated with several large-scale climatic features [*Murphy and Timbal*, 2008; *Ummenhofer et al.*, 2009; *Verdon-Kidd and Kiem*, 2009], such as the El Niño–Southern Oscillation, Indian Ocean Dipole, Southern Annular Mode, and the subtropical ridge; recent rainfall reductions have been attributed to some of these features. A similar reduction in rainfall, which has been characterized by particularly large

reductions during winter, has also occurred in southwest Western Australia since the 1970s [*Bates et al.*, 2008; *Petrone et al.*, 2010]. In southeast Australia, the largest reductions in rainfall have occurred in autumn months [*Murphy and Timbal*, 2008; *Cai and Cowan*, 2008a; *Kiem and Verdon-Kidd*, 2010; *Potter et al.*, 2010; *Timbal et al.*, 2010]. This is significant for runoff generation as less rainfall in autumn leads to lower soil moisture at the start of the runoff generation season beginning in winter in the southern MDB.

[7] Since 1950, the annual mean surface air temperature of Australia has increased by 0.16°C per decade, accompanied by a decrease in cold days and nights and an increase in hot days and nights [*CSIRO and Bureau of Meteorology*, 2007]. The annual trend in MDB-wide average daily temperature from 1950 to 2009 (based on an analysis of the high-quality temperature data set from the *Bureau of Meteorology* [2010]) is slightly higher than this at 0.2°C per decade. The increase in maximum temperatures in southeast Australia is greater than the increase in minimum and average temperatures: mean annual daily maximum temperature has increased by 0.9°C since 1990, with increases seen in all seasons [*Timbal et al.*, 2010]. Considered separately from changes in other climate variables, these increases in temperature are expected to result in greater evapotranspiration and hence less runoff for the same amount of rainfall. *Cai and Cowan* [2008b] attributed the decline since 1950 in MDB inflow modeled by the Murray-Darling Basin Commission. They related monthly temperature residuals (i.e., after removing any temperature component associated with monthly rainfall) to monthly inflow residuals. Using this method, they showed that the decline in annual rainfall accounts for 33% of the total decline in MDB inflow since 1950, and the increase in maximum temperatures accounts for 27%. However, it is not clear what hydrological or subannual climate processes related to increased temperatures are responsible for such a large reduction in runoff [*Kiem and Verdon-Kidd*, 2010].

[8] A number of studies have noted that the low annual rainfall occurring during the recent drought in southeast Australia has been accompanied by a decrease in interannual variability [*Nicholls*, 2006; *Murphy and Timbal*, 2008; *Bureau of Meteorology*, 2008]. That is, the recent drought has been characterized by consistently low annual rainfall, especially compared to the World War II drought [*Potter et al.*, 2010]. The lack of any high rainfall years is expected to decrease mean annual runoff due to the nonlinearity of the annual rainfall-runoff response, as well as potentially depleting surface and groundwater reservoirs. Changes in rainfall and potential evapotranspiration variability at other time scales may have also been responsible for changes in annual runoff in southeast Australia. *Verdon-Kidd and Kiem* [2009] examined the distribution of daily rainfall amounts in southeast Australia and showed that the intensity of autumn rainfall events has also decreased. Potentially, changes in the covariability of rainfall and potential evapotranspiration and daily rainfall sequencing may also be important.

1.3. Overview of the Study

[9] Although there has been much speculation, little work has been done on quantifying the relative roles of the hydroclimatic features of the recent drought in reducing runoff in the southern MDB. We chose to examine runoff reductions in the Campaspe river basin, shown in Figure 1, in which the annual rainfall and runoff reductions over 1997–2008 (see Table 1) are typical of the largest reductions in modeled annual runoff in the southern MDB over 1997–2008 [see *Chiew et al.*, 2010; *Potter et al.*, 2010, Table 1]. We define a number of scenarios in order to estimate the effect of a return to historical conditions of the mean and variability of rainfall and potential evapotranspiration climate inputs. As noted before, relatively simple semiempirical approaches to estimating runoff sensitivity are unable to estimate the effect of anything more than differences in annual rainfall. Investigating the effect of other hydroclimatic features requires a more detailed model, and in this study we use the SIMHYD rainfall-runoff model for this. For each scenario considered, we modify the climate input time series during 1997–2008 so they resemble the long-term climate data in mean and variability and then compare the resulting runoff to baseline (observed) runoff. The scenarios, described in sections 2.2 and 2.3, are intended to quantify the effect of the hydroclimatic features of the recent drought identified in section 1.2.

[10] The modeled runoff used here is generally reliable because the models are calibrated against reasonable amounts of gauged streamflow data in the high runoff generation areas [*Chiew et al.*, 2009b; *Vaze et al.*, 2010]. As the rainfall-runoff model is calibrated against a fixed time period, the parameter values represent land use over this period, and so the model does not account for other drivers of runoff (in particular, afforestation, deforestation, changes in vegetation response, and farm dams). This is not to say that changes in land use and possible nonstationarities in dominant hydrological processes have no effect on streamflow, but the temporal variability of the runoff response considered in this study is solely attributable to changes in climate inputs. In other words, the purpose of this study is to account for the unusually large reduction in modeled runoff, which is currently guiding water resource decision making in the Murray-Darling Basin [*CSIRO*, 2008b; *Murray-Darling Basin Authority*, 2010], with observed changes in the climate input time series.

[11] In section 2.1, we describe the climate data as well as the runoff data and SIMHYD model. The scenarios are described in sections 2.2 and 2.3. First, we describe the scenarios that consist of direct modifications of the observed 1997–2008 climate inputs, which are called "scaled drought" scenarios. Next, we describe scenarios that estimate the effect of changes in climate input variability, which are called "historical variability" scenarios. These historical variability scenarios consist of modifications of historical 12 year blocks of climate data. Averaged annual runoff for each scenario is presented in section 3, and we provide interpretations for the cause of the extra runoff resulting from each scenario. Section 4 provides discussion, and we end with conclusions.

2. Data and Methods

2.1. Climate and Runoff Data

[12] The climate data used for this study are based on the data set for southeast Australia described by *Chiew et al.*

[2009b], updated to the end of 2008. The source of the daily rainfall data is the SILO 0.05° (~5 km) grid cell data [*Jeffrey et al.*, 2001], which contain rainfall data interpolated from measurements made by the Australian Bureau of Meteorology. Areal potential evapotranspiration (PET) is calculated using Morton's wet environment evapotranspiration algorithms [*Morton*, 1983; *Chiew et al.*, 2009b].

[13] The daily runoff data come from rainfall-runoff modeling across southeast Australia using the SIMHYD daily lumped conceptual rainfall-runoff model [*Chiew et al.*, 2009b]. The model was calibrated against observed streamflow data from 219 medium-sized (50–2000 km^2) unregulated catchments over 1975–2006. Thus, the modeled runoff reflects the runoff response to rainfall and PET for a fixed 1975–2006 catchment condition. In particular, historical runoff is modeled as if historical land use was identical to current land use practices. Means, differences, and trends in annual rainfall, potential evapotranspiration, and runoff for the Campaspe are shown in Table 1.

[14] The modeled runoff in the high runoff-generating areas of the MDB is generally reliable as there are many gauged catchments there to calibrate the model, and modeling with several other rainfall-runoff models also gave similar runoff estimates [*Chiew et al.*, 2009b]. Modeling results in the Campaspe are very good, with verification Nash-Sutcliffe efficiency greater than 0.8 in all streamflow gauges in the upper Campaspe and little to no bias [*Chiew et al.*, 2008; *Vaze et al.*, 2010]. This gives us excellent confidence in the SIMHYD model's ability to reproduce runoff in the study region. In this study, we also calculated the runoff reduction and its causes using the Sacramento rainfall-runoff model [*Burnash et al.*, 1973], with almost identical results (not shown here).

2.2. Scaled Drought Scenarios

[15] In this section, we describe the climate scenarios that are intended to model the effect of observed differences in the mean of the climate inputs in the Campaspe over 1997–2008. Label the daily observed rainfall, potential evapotranspiration, and runoff data as $P_{d,m,y}$, $\mathrm{PET}_{d,m,y}$, and $Q_{d,m,y}$. Time series of scenario data are labeled by placing the abbreviation of the scenario name as a superscript.

2.2.1. Baseline Scenario

[16] This scenario simply uses the observed rainfall and potential evapotranspiration time series as described in section 2.1. We write

$$\bar{Q}_D^{\mathrm{BL}} = \frac{1}{12}\sum_{y\geq 1997} Q_{d,m,y}$$

for mean annual runoff during 1997–2008 calculated from these climate inputs. This is the baseline (BL) from which any increases in runoff resulting from the other scenarios is measured.

2.2.2. Annually Scaled Rainfall Scenario

[17] First, to estimate the effect of a return to historical (i.e., predrought) mean annual rainfall levels, with everything else held constant, we scale the daily rainfall time series for each grid cell so that the annual mean of the scaled time series over 1997–2008 is equal to the historical annual mean. So, first, calculate the historical annual mean of rainfall (for each grid cell):

$$\bar{P}_H = \frac{1}{102}\sum_{y<1997} P_{d,m,y}.$$

The denominator of the fraction is 102 as there are 102 whole years from 1895 to 1996. Also, calculate the mean annual rainfall during the drought:

$$\bar{P}_D = \frac{1}{12}\sum_{y\geq 1997} P_{d,m,y};$$

then, scaled potential (SP) rainfall is given by

$$P_{d,m,y}^{\mathrm{SP}} = \begin{cases} P_{d,m,y}, & y < 1997, \\ (\bar{P}_H/\bar{P}_D)P_{d,m,y}, & y \geq 1997, \end{cases}$$

and so the annual mean of $P_{d,m,y}^{\mathrm{SP}}$ from 1997 to 2008 is

$$\bar{P}_D^{\mathrm{SP}} = \bar{P}_H.$$

SP potential evapotranspiration is left unchanged:

$$\mathrm{PET}_{d,m,y}^{\mathrm{SP}} = \mathrm{PET}_{d,m,y}.$$

Mean annual SP scenario runoff over 1997–2008, $\bar{Q}_D^{\mathrm{SP}}$, is then calculated from these climate inputs.

2.2.3. Seasonally Scaled Rainfall Scenario

[18] As we saw in section 1.2, the southern MDB has seen a larger proportional reduction in rainfall during the autumn and winter months, and it has been suggested that this has contributed to the large reduction in streamflow. We estimate the effect on runoff of a return of the seasonality of rainfall to the predrought seasonality with the seasonally scaled rainfall scenario (SSP). First, calculate the monthly means of rainfall using the historical (predrought) data:

$$\bar{P}_{m=n,H} = \frac{1}{102}\sum_{m=n,y<1997} P_{d,m,y}$$

for $n = 1, \ldots, 12$. Similarly, calculate the monthly means of rainfall during the drought:

$$\bar{P}_{m=n,D} = \frac{1}{12}\sum_{m=n,y\geq 1997} P_{d,m,y}.$$

Then,

$$P_{d,m,y}^{\mathrm{SSP}} = \begin{cases} P_{d,m,y}, & y < 1997, \\ \left(\dfrac{\bar{P}_{m=1,H}}{\bar{P}_{m=1,D}}\dfrac{\bar{P}_D}{\bar{P}_H}\right)P_{d,1,y}, & m = 1, \quad y \geq 1997, \\ \vdots & \\ \left(\dfrac{\bar{P}_{m=12,H}}{\bar{P}_{m=12,D}}\dfrac{\bar{P}_D}{\bar{P}_H}\right)P_{d,12,y}, & m = 12, \quad y \geq 1997. \end{cases}$$

In this way,

$$\bar{P}_{m=n,D}^{\mathrm{SSP}} = \bar{P}_{m=n,H}\frac{\bar{P}_D}{\bar{P}_H}$$

for $n = 1, \ldots, 12$. So the monthly means of SSP rainfall after 1997 are a constant proportion of the predrought (historical) monthly means. The annual mean of SSP rainfall is equal to the mean annual rainfall during the drought:

$$\bar{P}_D^{\mathrm{SSP}} = \bar{P}_D.$$

As in the SP scenario, SSP potential evapotranspiration is left unchanged.

2.2.4. Annually Scaled Potential Evapotranspiration Scenario

[19] In order to estimate the effect of a return to predrought potential evapotranspiration (i.e., the extra runoff that would occur if mean annual potential evapotranspiration over 1997–2008 were equal to its historical value), we scale the potential evapotranspiration time series similarly to the way we scaled rainfall in the SP scenario:

$$\mathrm{PET}_{d,m,y}^{\mathrm{SPET}} = \begin{cases} \mathrm{PET}_{d,m,y}, & y < 1997, \\ (\overline{\mathrm{PET}}_H / \overline{\mathrm{PET}}_D)\mathrm{PET}_{d,m,y}, & y \geq 1997. \end{cases}$$

Rainfall in the scaled potential evapotranspiration (SPET) scenario is left unchanged. There is no seasonally scaled potential evapotranspiration scenario as during testing we found that there was practically no difference between such a scenario and the SPET scenario. This was because the effect from PET was found to be relatively small, and the changes in PET are not significantly different from season to season.

2.2.5. Interaction of Scenarios

[20] We also combine the above scenarios to estimate any interaction between the individual effects. The SP.SSP scenario combines the annually scaled scenario and the seasonally scaled scenario, which results in

$$P_{d,m,y}^{\mathrm{SP.SSP}} = \begin{cases} P_{d,m,y}, & y < 1997, \\ \dfrac{\bar{P}_{m=1,H}}{\bar{P}_{m=1,D}} P_{d,1,y}, & m = 1, \quad y \geq 1997, \\ \vdots & \\ \dfrac{\bar{P}_{m=12,H}}{\bar{P}_{m=12,D}} P_{d,12,y}, & m = 12, \quad y \geq 1997, \end{cases}$$

so that the monthly means of SP.SSP rainfall after 1997 are equal to the predrought (historical) rainfall monthly means,

$$\bar{P}_{m=n,D}^{\mathrm{SP.SSP}} = \bar{P}_{m=n,H},$$

and the mean annual SP.SSP rainfall after 1997 is equal to the historical mean annual rainfall,

$$\bar{P}_D^{\mathrm{SP.SSP}} = \bar{P}_H.$$

Figure 3 provides a graphical demonstration of the difference between means of BL, SP, SSP, and SP.SSP scenario rainfall. Any extra runoff from the SP.SSP over and above the sum of extra runoff from the SP and SSP scenarios individually is due to the interaction of the two scenarios.

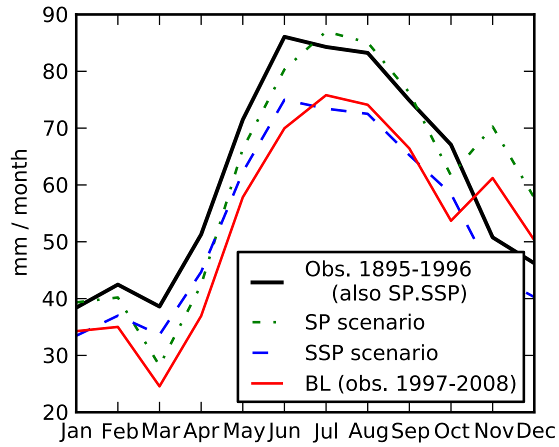

Figure 3. Average monthly rainfall for an example grid cell under different scenarios.

[21] We construct the SP.SPET scenario by scaling rainfall as described in the SP scenario above and scaling potential evapotranspiration as described in the SPET scenario. The remaining two interaction scenarios, SSP.SPET and SP.SSP.SPET, are constructed in analogous ways. Any increase in runoff from interaction scenarios over BL runoff is due to the combined effects of the scenarios. Runoff from an interaction scenario can be larger than the sum of runoff from the component scenarios individually, and this indicates a hydrological interaction between the two scenarios. If, in contrast, the increase in runoff from an interaction scenario is equal to the sum of the increases in runoff from the component scenarios, then the two effects would be considered to be independent.

2.3. Historical Variability Scenarios

[22] The preceding (scaled drought) scenarios described in section 2.2 use scaled daily time series of 1997–2008 rainfall and PET only. Runoff from these scenarios can be considered as runoff that would have occurred in 1997–2008 had the monthly or annual means of the observed daily time series been equal to the long-term averages. To consider the effect of interannual variability, submonthly variability, and potential changes in rainfall sequences, we construct additional scenarios, which we call the "historical variability" scenarios. To construct the historical variability scenarios, we replace 1997–2008 climate data with historical 12 year blocks of scaled climate data (i.e., the 91 blocks from 1895–1906 to 1985–1996). In this way, we use the variability inherent in the historical climate input time series to estimate the effect of any potential differences in variability that may have occurred during the recent drought. In contrast to the scaled drought scenarios, there will be 91 time series for each historical variability scenario.

2.3.1. Historical Variability Baseline Scenario

[23] The rainfall and potential evapotranspiration time series in the historical variability baseline (HVBL) scenario is constructed to have monthly means of rainfall and mean annual potential evapotranspiration over 1997–2008 equal to the means from the BL scenario. In this way, any difference in runoff occurring from this scenario must be due to differences in rainfall or PET at different (smaller than

monthly or larger than annual) time scales. Specifically, we construct the ith HVBL rainfall time series as

$$P_{d,m,y}^{\mathrm{HVBL}(i)} = \begin{cases} P_{d,m,y}, & y < 1997, \\ \dfrac{\bar{P}_{m=1,D}}{\bar{P}_{m=1,1894+i\le y\le 1905+i}} P_{d,1,y-103+i}, & m=1,\ y\ge 1997, \\ \vdots & \\ \dfrac{\bar{P}_{m=12,D}}{\bar{P}_{m=12,1894+i\le y\le 1905+i}} P_{d,12,y-103+i}, & m=12,\ y\ge 1997, \end{cases}$$

for $i = 1,\ldots, 91$, which corresponds to 12 year blocks of rainfall of 1895–1906 to 1985–1996. Here $\bar{P}_{m=n,1894+i\le y\le 1905+i}$ is the average rainfall of the nth month taken over the years $1894 + i$ to $1905 + i$. This is illustrated schematically in Figure 4. Figure 4 (top) shows BL rainfall for the two time periods 1955–1966 and 1997–2008 (in this example, $i = 61$). Figure 4 (bottom) shows the scaled block of 1955–1966 rainfall replacing the 1997–2008 rainfall data for HVBL(i). This scaling makes the monthly means of each HVBL(i) time series from 1997 to 2008 equal to the monthly mean rainfall of observed rainfall during the drought,

$$\bar{P}_{m=n,D}^{\mathrm{HVBL}(i)} = \bar{P}_{m=n,D},$$

and so the annual mean of HVBL(i) rainfall is equal to the annual mean of observed rainfall during the drought as well:

$$\bar{P}_{D}^{\mathrm{HVBL}(i)} = \bar{P}_{D}.$$

Potential evapotranspiration for the HVBL(i) scenario is scaled so that the annual mean from 1997 to 2008 is equal to the annual mean of observed PET during the drought:

$$\mathrm{PET}_{d,m,y}^{\mathrm{HVBL}(i)} = \begin{cases} \mathrm{PET}_{d,m,y}, & y < 1997, \\ \left(\overline{\mathrm{PET}}_D / \overline{\mathrm{PET}}_{1894+i\le y\le 1905+i}\right)\mathrm{PET}_{d,m,y=103+i}, & y \ge 1997. \end{cases}$$

From here we use the HVBL(i) rainfall and potential evapotranspiration inputs to calculate HVBL(i) runoff: $\bar{Q}_D^{\mathrm{HVBL}(i)}$. We then take HVBL scenario runoff as the average 1997–2008 mean annual runoff over all 91 HVBL(i) time series:

$$\bar{Q}_D^{\mathrm{HVBL}} = \left(\sum_{i=1}^{91} \bar{Q}_D^{\mathrm{HVBL}(i)}\right) \Big/ 91.$$

2.3.2. Other HV Scenarios

[24] The remaining HV scenarios are constructed identically to the methods described in section 2.2. That is, we simply scale each HVBL(i) time series as if it were the BL time series. In this way we obtain the HVSP, HVSSP, HVSPET, HVSP.SSP, HVSP.SPET, HVSSP.SPET, and HVSP.SSP.SPET scenarios. Differences between the HV scenarios and the corresponding scaled drought scenarios (e.g., between HVSP and SP) are due to the interaction between differing historical variability in climate inputs and the effect captured in the scaled drought scenario. Finally, the effect on runoff of variability in antecedent (i.e., predrought) moisture conditions was estimated by replacing each 12 year block of historical rainfall and PET with BL data and calculating the resulting 12 year mean annual runoff. This effect was insignificant, and so not considered further: mean annual runoff averaged over all 12 year blocks was less than 0.1% greater than BL runoff.

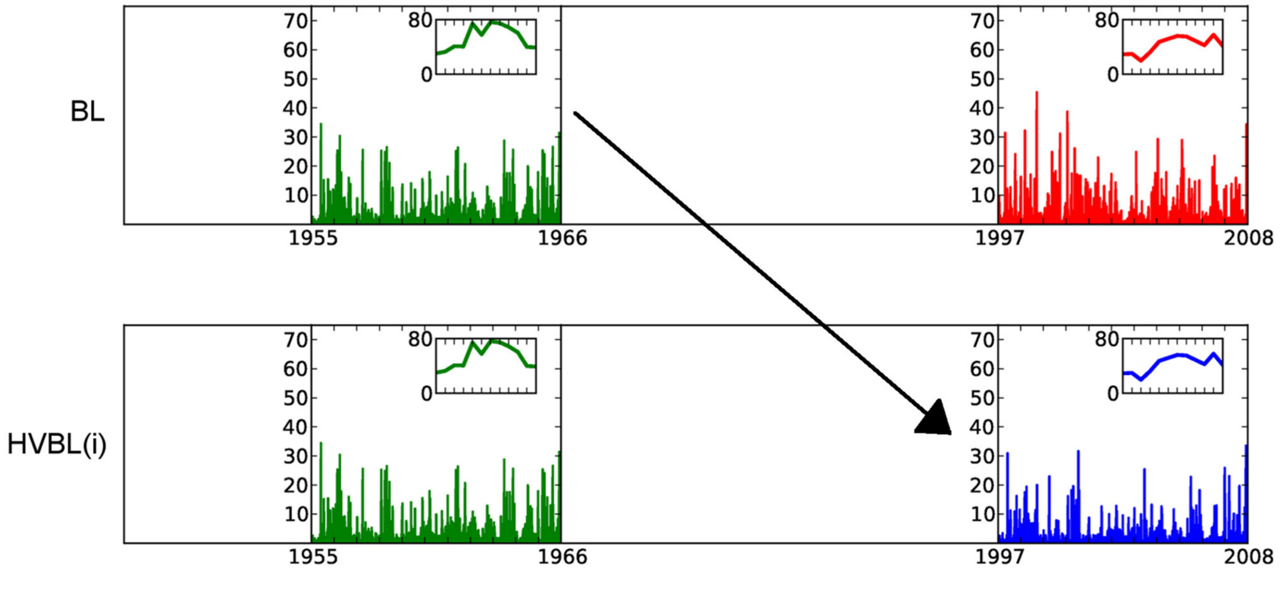

Figure 4. Schematic diagram for historical variability baseline (HVBL) rainfall transformation period. Inset axes are monthly rainfall means.

3. Results

3.1. Rainfall and Runoff Reductions From the Baseline Scenario

[25] Mean annual rainfall and runoff in the Campaspe (based on the modeled data used here) are $\bar{P}_H = 602$ mm and $\bar{Q}_H = 68.0$ mm over 1895–1996 and $\bar{P}_D = 513$ mm and $\bar{Q}_D = 28.1$ mm over 1997–2008, or a 15% and 59% reduction from the long-term mean (Table 1). The reductions over the recent drought are often compared to the World War II drought [e.g., *Murphy and Timbal*, 2008; *Verdon-Kidd and Kiem*, 2009; *Potter et al.*, 2010]. In the Campaspe, the 12 year running means of annual rainfall and runoff are lowest around that time during 1937–1948, with rainfall and runoff 499 and 43.0 mm (17% and 37% reduction from the means over 1895–1996). Note that compared to the 1997–2008 period, the percentage reduction in mean annual rainfall over 1937–1948 from the long-term is slightly higher, and yet the percentage reduction in mean annual runoff is considerably lower.

3.2. Scenario Runoff

[26] The runoff column in Table 2 shows mean annual runoff over 1997–2008 for each of the scenarios ($\bar{Q}_D^{\mathrm{BL}}$, $\bar{Q}_D^{\mathrm{SP}}$, $\bar{Q}_D^{\mathrm{HVBL}}$, $\bar{Q}_D^{\mathrm{HVSP}}$, etc.). The increase column is scenario runoff minus BL runoff. The column labeled extra shows the extra runoff contribution from the scenario individually (for example, the extra increase from the SP.SPET scenario is the SP.SPET increase minus the sum of extra increases from the SP and SPET scenarios). The proportion column is the ratio of the extra runoff from each scenario to the reduction in runoff over 1997–2008 of 39.9 mm. The total runoff from the HVSP.SSP.SPET scenario, i.e., from all treatments of the climate input time series applied simultaneously, is 61.3 mm, accounting for 83% of the observed runoff reduction over 1997–2008.

3.2.1. Runoff From Scaled Drought Scenarios

[27] Runoff from the SP scenario explains the single largest individual proportion (52%) of the observed runoff reduction. This increase in runoff from SP of 20.6 mm is similar in magnitude but somewhat lower than the "expected" runoff reduction of 26.5 mm (i.e., a 39% reduction from the long-term runoff of 68.0 mm) based on the elasticity-based estimate described in section 1.1. Significant extra runoff is produced from the SSP scenario (6% of the observed runoff reduction), the SP.SSP scenario (5%), the SPET scenario (3%), and the SP.SPET scenario (2%). The additional effects from the two other interaction scenarios (SSR.SPET and SR.SSR.SPET) are negligible. Any interaction between the different scaled drought scenarios appears to have been captured in the SP.SSP and SP.SPET scenarios.

[28] Extra runoff from the SSP scenario comes from more rainfall occurring in autumn and winter (Figure 3) and thus provides a measure of the effect of changed rainfall seasonality. Extra runoff from SPET is due to a reduction in PET compared to BL. The runoff effects from the SSP and SPET scenarios are increased by approximately 80% and two thirds when each scenario interacts with the SP scenario, i.e., when combined with greater mean annual rainfall. For example, the increase in runoff of 24.9 mm from scenario SP.SSP is larger than the sum of the extra runoff from the SP and SSP scenarios individually, and this occurs because the absolute volume (in mm) of more rainfall in autumn and winter is larger when combined with an increase in mean annual rainfall. Similarly, the extra runoff from the SP.SPET scenario is due to the interaction of decreased potential evapotranspiration with increased annual rainfall. This is because the decrease in potential evapotranspiration leads to comparatively increased soil moisture, and so the increase in rainfall is more likely to result in more runoff production.

3.2.2. Runoff From Historical Variability Scenarios

[29] Averaged runoff from the HV scenarios is always larger than runoff from the corresponding scaled scenarios (see Table 2). In particular, averaged HVBL runoff is 3.5 mm larger than BL runoff. This corresponds to 9% of the observed runoff reduction and is the largest amount of extra runoff from any individual scenario after SP. Runoff from the HVSP scenario is 26.5 mm larger than BL runoff, and when we subtract the individual increases from the components of HVSP, namely, SP and HVBL, we are left with a 2.4 mm increase attributable directly to the interaction

Table 2. Mean Annual 1997–2008 Runoff in the Campaspe River Basin Under Different Scenarios

Scenario	Interpretation	Runoff (mm)	Increase (mm)	Extra (mm)	Proportion
BL (1997–2008)		28.1			
Long term (1895–1996)		68.0	39.9		
SP	return to historical mean annual rainfall	48.7	20.6	20.6	52%
SSP	return to historical rainfall seasonality	30.5	2.4	2.4	6%
SPET	return to historical mean annual potential evapotranspiration	29.2	1.1	1.1	3%
SP.SSP	changed seasonality of rainfall at historical mean annual rainfall	53.0	24.9	1.9	5%
SP.SPET	decreased PET at historical mean annual rainfall	50.6	22.5	0.8	2%
SSP.SPET		31.8	3.7	0.2	1%
SP.SSP.SPET		55.0	26.9	−0.1	0%
HVBL	return to historical rainfall variability	31.6	3.5	3.5	9%
HVSP	increased rainfall variability at historical mean annual rainfall	54.6	26.5	2.4	6%
HVSSP		34.3	6.2	0.3	1%
HVSPET		32.8	4.7	0.1	0%
HVSP.SSP		59.1	31.0	−0.1	0%
HVSP.SPET		56.6	28.5	0.0	0%
HVSSP.SPET		35.7	7.6	0.0	0%
HVSP.SSP.SPET	all scenarios combined	61.3	33.2	0.1	0%
Total				33.2	83%

between HVBL and SP. This accounts for 6% of the observed reduction. In a similar way to the SSP and SPET scenarios, we see that the effect on runoff of changed variability is increased by about two thirds when combined with an increase in annual rainfall to historical levels. All other HV interaction scenarios produce negligible extra runoff. The extra runoff from the HVBL scenario can be attributed to rainfall and PET variability at submonthly and interannual time scales. Specifically, this could include the interannual variability of rainfall, the daily rainfall distribution, the covariability of rainfall and PET, or the rainfall sequencing.

[30] In order to explore which aspects of climate variability are responsible for HVBL runoff, we regress the time series of $\bar{Q}_D^{\mathrm{HVBL}(i)}$ for $i = 1, \ldots, 91$, against different measures of climate input variability. The variables chosen are (1) standard deviation of annual rainfall, (2) proportion of wet days (defined as any day with rainfall over 0 mm), and (3) proportion of very wet days (rainfall over 30 mm) for the HVBL(i) rainfall data over 1997–2008. Additional variables considered for the regression were the covariance between rainfall and PET, other measures of the distribution of daily rainfall, and the mean and variance of wet and dry spell lengths. Some of these were found to be slightly related to $\bar{Q}_D^{\mathrm{HVBL}(i)}$, but the main features of $\bar{Q}_D^{\mathrm{HVBL}(i)}$ in Figure 5 were accounted for using the three predictor variables above.

[31] The solid line in Figure 5a shows $\bar{Q}_D^{\mathrm{HVBL}(i)}$, and the dashed line represents $\bar{Q}_D^{\mathrm{HVBL}(i)}$ averaged over $i = 1, \ldots, 91$ of 31.6 mm (which is the value for HVBL averaged runoff in Table 2). The dotted line in Figure 5a is the predicted time series from the multiple linear regression between $\bar{Q}_D^{\mathrm{HVBL}(i)}$ and the three predictor variables described above, which in Figures 5b–5d are scaled according to their significance to the regression (i.e., relative magnitude of partial sum of squares in Table 3).

[32] From Figure 5, we see clearly that the standard deviation of annual rainfall accounts for most of the variability in $\bar{Q}_D^{\mathrm{HVBL}(i)}$ (see also sum of squares results in Table 3). The nonlinear relationship between annual rainfall and runoff means that 12 year sequences with high interannual variability of rainfall produce more runoff than sequences with lower interannual variability as the higher rainfall years produce more than enough runoff to compensate for the reduction in runoff in low rainfall years. This explains the large peak in HVBL runoff around the 1930s to 1940s. In fact, observed runoff during 1937–1948 of 43.0 mm is close to the maximum of HVBL runoff around this time, so this suggests that larger interannual variability of rainfall is the main reason why annual runoff during the World War II Drought was comparatively higher than during the recent drought. The decreasing trend of wet days since the 1960s (Figure 5c) means that soil moisture would likely be lower, and so any rainfall that does fall results in less runoff and is associated with a lowering of HVBL runoff in recent decades. An apparent increase in the proportion of very wet days since the 1930s to 1940s (Figure 5d) would tend to increase HVBL runoff. However, it seems that most of this effect is encompassed in the annual standard deviation variable (as indicated by the large difference between sequential and partial sum of squares in Table 3 when the wet days variable is fitted first).

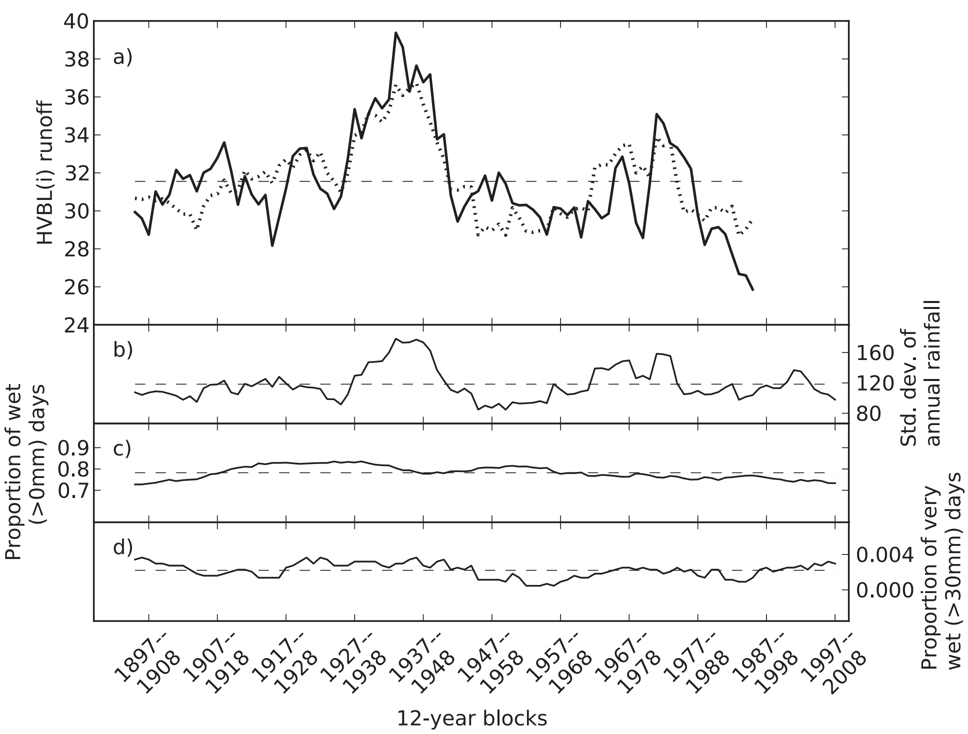

Figure 5. (a) Progression of HVBL(i) runoff averaged over 1997–2008 (solid line) and predicted by the regression (dotted line). (b–d) The independent (predictor) climate variables used in the regression. These are scaled in accordance to their contribution to the regression (see Table 3).

Table 3. Summary Statistics for the Multiple Linear Regression of HVBL(i) Runoff Against Selected Climate Variables

Variable	Coefficient	Standard Error	t Statistic	p Value	Sequential Sum of Squares	Partial Sum of Squares
Intercept	6.5	4.8	1.4	0.18		
Proportion of very wet days	8.0×10^2	2.2×10^2	3.6	5.0×10^{-4}	158.5	35.5
SD of annual rainfall	6.9×10^{-2}	8.4×10^{-3}	8.2	$<10^{-4}$	185.0	186.1
Proportion of wet days	1.9×10^1	5.9	3.2	1.7×10^{-3}	29	29

Statistic	Value
R^2	0.608
Adjusted R^2	0.595
Prediction sum of squares R^2	0.574
Sum of squared residual	239.9
F statistic of regression	45
p value of regression	$<10^{-6}$
Root-mean-square error	1.66

[33] The results provide an estimate for the quantification of some of the effects on runoff of the hydroclimatic features of the recent drought. Extra runoff produced from the SSP, SPET, and HVBL scenarios estimate the effect of a return to historical conditions of rainfall seasonality, potential evapotranspiration, and interannual variability. When combined with the SP scenario, the effects of the SPET and HVBL scenario are both increased by approximately two thirds, while SSP increases by around 80%. Thus, the sensitivity of runoff to changes in rainfall and potential evapotranspiration seems to be higher in wetter years and lower in drier years. Recall from section 3.2.1 that the SP scenario was somewhat less than the expected reduction in runoff estimated using the median-based elasticity. This may be because the SP scenario estimates the effect from the drought baseline, whereas elasticities are generally calculated for mean conditions. This is consistent with the findings of *Fu et al.* [2007], who demonstrated the dependence of the elasticity of runoff on annual rainfall and temperature, in contrast to previous studies that have assumed that the elasticity of runoff of a catchment is a constant [e.g., *Sankarasubramanian et al.*, 2001].

[34] Including the effect of a return to historical mean annual rainfall, we estimate that lower interannual variability of rainfall during the drought accounts for 15% of the observed runoff reduction in the Campaspe river basin. Changed rainfall seasonality accounts for 11% of the reduction, and increased potential evapotranspiration accounts for 5%. The residual reduction (17% of the observed reduction) is due to climatic variability in the climate input time series that is not captured by the scenarios. Note that part of this residual may be due to the apparent lower sensitivity of runoff from the drought baseline discussed above.

4. Discussion

[35] The scaling method used in the SP and SSP scenarios does not consider changes in the shape of the daily rainfall distribution. A more complicated scaling method might scale large rainfall events differently to small rainfall events. Any changes during the drought in the relative frequency of high and low rainfall events could potentially not be captured by the rainfall scaling scenarios. Thus, the scaling method used to construct the scenarios may underestimate the occurrence of hydrologically important large daily rainfall events. *Mpelasoka and Chiew* [2009] compared the differences in modeled runoff occurring from GCM rainfall projections using both the constant scaling method in the scenarios described in section 2 and a rainfall scaling method that alters the daily rainfall distribution (i.e., high and low rainfall events are scaled differently). They found that for southeast Australia, changes in annual rainfall of ±15% resulted in differences in annual runoff between the two methods of less than 5%. This may be one component of the residual reduction.

[36] The effect of increased PET is smaller than the two other factors identified (i.e., increased variability and changed rainfall seasonality). Other studies [e.g., *Cai and Cowan*, 2008b; *Yu et al.*, 2010] have found that increased temperatures had an effect approximately equal in magnitude to the effect from decreased rainfall in the MDB since 1950. As these studies are empirical/statistical studies, the relationships developed between residual temperature and inflow may, in fact, be incorporating some of the subannual and interannual changes in rainfall identified here. That is to say, if changed rainfall seasonality or variability are linked, either causally or simply associatively, with increased temperatures, the above studies may be incorporating these with any temperature effect.

[37] Disregarding indirect effects of near-surface air temperature on runoff (e.g., causal or associative relationships between regional rainfall and changing temperatures), the only way increasing temperatures can influence runoff in a calibrated rainfall-runoff model is through consequent changes in potential evapotranspiration. In this study, Morton's areal (wet environment) potential evapotranspiration in the Campaspe as estimated from the SILO climate data increased during the recent drought (Table 1), which is consistent with projections of increasing areal potential evapotranspiration in the future [*CSIRO and Bureau of Meteorology*, 2007]. However, pan evaporation has been decreasing globally even though air temperatures have generally been increasing, a phenomenon known as the "pan evaporation paradox" [e.g., *Roderick et al.*, 2009]. Over most of the rest of Australia, pan evaporation and Penman potential evaporation has decreased, which is primarily explained by a trend of decreasing wind speed or regional "stilling," which has been seen to approximately offset the positive effect of increasing temperatures [*Roderick et al.*, 2007; *McVicar et al.*, 2008; *Donohue et al.*, 2010a].

However, estimates of Penman potential evaporation in the MDB have been increasing slightly in the last few decades, as a decrease in vapor pressure associated with lower regional rainfall has approximately compensated for the decrease in wind speed [*McVicar et al.*, 2010]. And yet, if any stilling effect were included in the formulation of potential evapotranspiration used in this study, the increase in potential evapotranspiration would be relatively less, and so the effect on runoff of the SPET scenario should be less. As such, in light of evidence for regional stilling, we can consider the effect from the SPET scenario to be an upper bound for the direct effect of increased temperature on runoff.

[38] Changes in land use and vegetation were not considered in this study as we have looked solely at the effect on runoff of differences in climate inputs. This study looked at the runoff generation process and how differences in recent climate inputs were likely to affect runoff on the basis of the historical rainfall-runoff response. Indeed, the purpose of using a rainfall-runoff model was to isolate the rainfall-runoff process from any land use change effects in the observed streamflow signal from the unimpaired streamflow gauges located in the Campaspe river basin. In terms of reproducing unimpaired streamflow, the modeling results in the Campaspe are among the most accurate in the MDB [*CSIRO*, 2008a] because of the relatively high number of gauged catchments in the study area. The estimates of the effect of differences in recent climate inputs on runoff are necessarily dependent on model assumptions, but we nevertheless have confidence in the results as the proportion of observed runoff reduction explained by the different scenarios was within $\pm 1\%$ of the results using the Sacramento model. By calibrating the models to the 1975–2006 time period, we are assuming a fixed catchment condition. In reality, land use and vegetation may have been different in the past. However, as we are comparing recent to historical modeled runoff, in which the parameters are held constant and hence land use is assumed to be unchanged from the recent past, the HV results give the estimated runoff from historical climate inputs in the presence of current catchment conditions. In light of the very good model validation results in the Campaspe [*CSIRO*, 2008a], we consider that the historical modeled runoff is very close to the historical observed runoff, especially at the annually aggregated scale.

[39] In terms of vegetation changes, empirical studies have shown that mean annual evapotranspiration is at least partially related to vegetation cover and type [*Zhang et al.*, 2001; *Oudin et al.*, 2008; *Donohue et al.*, 2010b; *Peel et al.*, 2010], and this vegetation information is expected to be encoded in the rainfall-runoff model calibration procedure. However, *Donohue et al.* [2010b] showed that interannual variability of evapotranspiration and streamflow at catchment and regional scales in Australia is primarily related to interannual variability of rainfall and consequent changes in catchment water storage. Clearly, vegetation is important to this, but the role of vegetation dynamics is less easily identifiable, at least in the steady state model considered by *Donohue et al.* [2010b].

[40] There has also been some speculation on the effect on runoff of vegetation response to enhanced CO_2, as well as potential changes in surface-subsurface connectivity and other dominant hydrological processes in a warmer climate [*Gedney et al.*, 2006; *Cai and Cowan*, 2008b; *Cai et al.*, 2009; *Chiew et al.*, 2009a; *Leblanc et al.*, 2009; *Cruz et al.*, 2010; *McVicar et al.*, 2010; *Petrone et al.*, 2010]. By its nature, the current modeling approach does not and cannot consider these changes. However, these are rarely considered in water resources applications because there is considerable uncertainty on how runoff will respond to these changes in landscape processes and surface-atmosphere feedbacks, and this is an area of considerable ongoing research.

5. Conclusion

[41] The large reductions in mean annual rainfall observed in many parts of southeast Australia since 1997 have not been large enough to explain the much more severe reductions in mean annual runoff. The observed reduction in annual runoff during 1997–2008 in the Campaspe of 59% is much greater than the expected reduction of 39% based on the observed annual rainfall reduction of 15% and the long-term rainfall elasticity of runoff. Several reasons have been proposed for this much larger reduction, including a greater proportional reduction in autumn and winter rainfall, increased temperatures, and less interannual variability of rainfall. Using the SIMHYD rainfall-runoff model and scenarios of scaled 1997–2008 climate inputs and scaled historical climate input, we estimate that the reduction in mean annual rainfall accounts for 52% of the reduction in runoff in the Campaspe over 1997–2008; changed variability in climate inputs, principally less interannual variability of rainfall during the recent drought period, accounts for 15% of the observed runoff reduction; changed rainfall seasonality accounts for 11%, and increased potential evapotranspiration accounts for 5%. Thus, any direct effect from increasing temperatures (i.e., through increased potential evapotranspiration) is a relatively minor aspect of the runoff reduction and would be tempered by apparent decreases in wind speed. Changes in other hydroclimate processes related either causally or associatively with increasing temperatures may act to decrease runoff, however. The sensitivity of annual runoff to the three hydroclimatic features of the recent drought in the Campaspe is dependent on the level of annual rainfall. For example, we showed that a lowering of potential evapotranspiration has more effect on runoff during wetter years compared to drier years. Some uncertainty exists in the modeled results due to changes in farm dams and other land use changes. Current work is considering the effect of changes in groundwater and land use changes on the hydrological response of runoff to variability in climatic variables in southeast Australia.

[42] **Acknowledgments.** This work is supported by the South Eastern Australia Climate Initiative and the CSIRO Water for a Healthy Country National Research Flagship. The authors would like to thank Lu Zhang, David Post, Tim McVicar, and Randall Donohue, as well as Geoff Pegram and the anonymous journal reviewers, whose comments have significantly improved this paper. Additional assistance with the study was provided by Jin Teng, Jean-Michel Perraud, and Jai Vaze.

References

Bates, B. C., P. Hope, B. Ryan, I. Smith, and S. Charles (2008), Key findings from the Indian Ocean Climate Initiative and their impact on policy development in Australia, *Clim. Change*, *89*, 339–354, doi:10.1007/s10584-007-9390-9.

Bureau of Meteorology (2008), Long-term rainfall deficiencies continue in southern Australia while wet conditions dominate, *Spec. Clim. Statement 16*, Melbourne, Victoria, Australia. [Available at http://www.bom.gov.au/climate/current/statements/scs16.pdf.]

Bureau of Meteorology (2010), Australia's high-quality climate change datasets, Melbourne, Victoria, Australia. [Available at http://www.bom.gov.au/climate/change/datasets/datasets.shtml.]

Burnash, R. J. C., R. L. Ferral, and R. A. McGuire (1973), A generalized streamflow simulation system—Conceptual modelling for digital computers, report, Natl. Weather Serv., U.S. Dep. of Comm., Washington, D. C.

Cai, W., and T. Cowan (2008a), Dynamics of late autumn rainfall reduction over southeastern Australia, *Geophys. Res. Lett.*, *35*, L09708, doi:10.1029/2008GL033727.

Cai, W., and T. Cowan (2008b), Evidence of impacts from rising temperature on inflows to the Murray-Darling Basin, *Geophys. Res. Lett.*, *35*, L07701, doi:10.1029/2008GL033390.

Cai, W., T. Cowan, P. Briggs, and M. Raupach (2009), Rising temperature depletes soil moisture and exacerbates severe drought conditions across southeast Australia, *Geophys. Res. Lett.*, *36*, L21709, doi:10.1029/2009GL040334.

Chiew, F. H. S. (2006), Estimation of rainfall elasticity of streamflow in Australia, *Hydrol. Sci. J.*, *51*, 613–625.

Chiew, F. H. S., et al. (2008), Rainfall-runoff modelling across the Murray-Darling Basin, a report to the Australian Government from the CSIRO Murray-Darling Basin Sustainable Yields Project, 62 pp., Commonw. Sci. and Ind. Res. Organ., Canberra.

Chiew, F. H. S., W. Cai, and I. N. Smith (2009a), Advice on defining climate scenarios for use in the Murray-Darling Basin Authority Basin Plan modelling, *MDBA Publ. 33/09*, Murray-Darling Basin Auth., Canberra.

Chiew, F. H. S., J. Teng, J. Vaze, D. A. Post, J. M. Perraud, D. G. C. Kirono, and N. R. Viney (2009b), Estimating climate change impact on runoff across southeast Australia: Method, results, and implications of the modeling method, *Water Resour. Res.*, *45*, W10414, doi:10.1029/2008WR007338.

Chiew, F. H. S., W. J. Young, W. Cai, and J. Teng (2010), Current drought and future hydroclimate projections in southeast Australia and implications for water resources management, *Stochastic Environ. Res. Risk Assess.*, *4*, 601–612, doi:10.1007/s00477-010-0424-x.

Commonwealth Scientific and Industrial Research Organisation (CSIRO) (2008a), Water availability in the Campaspe, a report to the Australian Government from the CSIRO Murray-Darling Basin Sustainable Yields Project, 120 pp., Canberra.

Commonwealth Scientific and Industrial Research Organisation (CSIRO) (2008b), Water availability in the Murray-Darling Basin, a report to the Australian Government from the CSIRO Murray-Darling Basin Sustainable Yields Project, 67 pp., Canberra.

Commonwealth Scientific and Industrial Research Organisation (CSIRO) and Bureau of Meteorology (2007), Climate change in Australia, technical report, Canberra. [Available at http://www.climatechangeinaustralia.gov.au.]

Cruz, F. T., A. J. Pitman, and Y. Wang (2010), Can the stomatal response to higher atmospheric carbon dioxide explain the unusual temperatures during the 2002 Murray-Darling Basin drought?, *J. Geophys. Res.*, *115*, D02101, doi:10.1029/2009JD012767.

Donohue, R. J., T. R. McVicar, and M. L. Roderick (2010a), Assessing the ability of potential evaporation formulations to capture the dynamics in evaporative demand within a changing climate, *J. Hydrol.*, *386*, 186–197, doi:10.1016/j.jhydrol.2010.03.020.

Donohue, R. J., M. L. Roderick, and T. R. McVicar (2010b), Can dynamic vegetation information improve the accuracy of Budyko's hydrological model?, *J. Hydrol.*, *390*, 25–34, doi:10.1016/j.jhydrol.2010.06.025.

Dooge, J. C. I., M. Bruen, and B. Parmentier (1999), A simple model for estimating the sensitivity of runoff to long-term changes in precipitation without a change in vegetation, *Adv. Water Resour.*, *23*, 153–163.

Fu, G., S. P. Charles, and F. H. S. Chiew (2007), A two-parameter climate elasticity of streamflow index to assess climate change effects on annual streamflow, *Water Resour. Res.*, *43*, W11419, doi:10.1029/2007WR005890.

Gedney, N., P. M. Cox, R. A. Betts, O. Boucher, C. Huntingford, and P. A. Stott (2006), Detection of a direct carbon dioxide effect in continental river runoff records, *Nature*, *439*, 835–838, doi:10.1038/nature04504.

Jeffrey, S. J., J. O. Carter, K. B. Moodie, and A. R. Beswick (2001), Using spatial interpolation to construct a comprehensive archive of Australian climate data, *Environ. Modell. Software*, *16*, 309–330.

Kiem, A. S., and D. C. Verdon-Kidd (2010), Towards understanding hydroclimatic change in Victoria, Australia—Preliminary insights into the "Big Dry", *Hydrol. Earth Syst. Sci.*, *14*, 433–445, doi:10.5194/hess-14-433-2010.

Koster, R. D., and M. J. Suarez (1999), A simple framework for examining the interannual variability of land surface moisture fluxes, *J. Clim.*, *12*, 1911–1917.

Leblanc, M. J., P. Tregoning, G. Ramillien, S. O. Tweed, and A. Fakes (2009), Basin-scale, integrated observations of the early 21st century multiyear drought in southeast Australia, *Water Resour. Res.*, *45*, W04408, doi:10.1029/2008WR007333.

McVicar, T. R., T. G. Van Niel, L. T. Li, M. L. Roderick, D. P. Rayner, L. Ricciardulli, and R. J. Donohue (2008), Wind speed climatology and trends for Australia, 1975–2006: Capturing the stilling phenomenon and comparison with near-surface reanalysis output, *Geophys. Res. Lett.*, *35*, L20403, doi:10.1029/2008GL035627.

McVicar, T. R., R. J. Donohue, A. P. O'Grady, and L. T. Li (2010), The effects of climatic changes on plant physiological and catchment ecohydrological processes in the high-rainfall catchments of the Murray-Darling Basin: A scoping study, report, 95 pp., CSIRO Water for a Healthy Country National Research Flagship, Canberra.

Milly, P. C. D., and K. A. Dunne (2002), Macroscale water fluxes: 2. Water and energy supply control of their interannual variability, *Water Resour. Res.*, *38*(10), 1206, doi:10.1029/2001WR000760.

Morton, F. I. (1983), Operational estimates of areal evapotranspiration and their significance to the science and practice of hydrology, *J. Hydrol.*, *66*, 1–76.

Mpelasoka, F. S., and F. H. S. Chiew (2009), Influence of rainfall scenario construction methods on runoff projections, *J. Hydrometeorol.*, *10*, 1168–1183, doi:10.1175/2009JHM1045.1.

Murphy, B. F., and B. Timbal (2008), A review of recent climate variability and climate change in southeastern Australia, *J. Climatol.*, *28*, 859–879, doi:10.1002/joc.1627.

Murray-Darling Basin Authority (2010), Guide to the proposed basin plan: Overview, report, Canberra.

National Climate Centre (2010), Australia's wettest September on record but it is not enough to clear long-term rainfall deficits, *Spec. Clim. Statement 22*, Melbourne, Victoria, Australia. [Available at http://www.bom.gov.au/climate/current/statements/scs22.pdf.]

Nicholls, N. (2004), The changing nature of Australian droughts, *Clim. Change*, *63*, 323–336.

Nicholls, N. (2006), Detecting and attributing Australian climate change: A review, *Aust. Meteorol. Mag.*, *55*, 199–211.

Oudin, L., V. Andréassian, J. Lerat, and C. Michel (2008), Has land cover a significant impact on mean annual streamflow? An international assessment using 1508 catchments, *J. Hydrol.*, *357*, 303–316, doi:10.1016/j.jhydrol.2008.05.021.

Peel, M. C., T. A. McMahon, and B. L. Finlayson (2010), Vegetation impact on mean annual evapotranspiration at a global catchment scale, *Water Resour. Res.*, *46*, W09508, doi:10.1029/2009WR008233.

Petrone, K. C., J. D. Hughes, T. G. Van Niel, and R. P. Silberstein (2010), Streamflow decline in southwestern Australia, 1950–2008, *Geophys. Res. Lett.*, *37*, L11401, doi:10.1029/2010GL043102.

Potter, N. J., and L. Zhang (2009), Interannual variability of catchment water balance in Australia, *J. Hydrol.*, *369*, 120–129, doi:10.1016/j.jhydrol.2009.02.005.

Potter, N. J., F. H. S. Chiew, A. J. Frost, R. Srikanthan, T. A. McMahon, M. C. Peel, and J. M. Austin (2008), Characterisation of recent rainfall and runoff in the Murray-Darling Basin, a report to the Australian Government from the CSIRO Murray-Darling Basin Sustainable Yields Project, 40 pp., Commonw. Sci. and Ind. Res. Organ., Canberra.

Potter, N. J., F. H. S. Chiew, and A. J. Frost (2010), An assessment of the severity of recent reductions in rainfall and runoff in the Murray-Darling Basin, *J. Hydrol.*, *381*, 52–64, doi:10.1016/j.jhydrol.2009.11.025.

Roderick, M. L., L. D. Rotstayn, G. D. Farquhar, and M. T. Hobbins (2007), On the attribution of changing pan evaporation, *Geophys. Res. Lett.*, *34*, L17403, doi:10.1029/2007GL031166.

Roderick, M. L., M. T. Hobbins, and G. D. Farquhar (2009), Pan evaporation trends and the terrestrial water balance. I. Principles and observations, *Geogr. Compass*, *3*, 746–760, doi:10.1111/j.1749-8198.2008.00213.x.

Sankarasubramanian, A., R. M. Vogel, and J. F. Limbrunner (2001), Climate elasticity of streamflow in the United States, *Water Resour. Res.*, *37*, 1771–1781, doi:10.1029/2000WR900330.

Schaake, J. C. (1990), From climate to flow, in *Climate Change and U.S. Water Resources*, edited by P. E. Waggoner, chap. 8, pp. 177–206, John Wiley, New York.

Timbal, B., et al. (2009), The continuing decline in south-east Australian rainfall—Update to May 2009, *CAWCR Res. Lett.*, *2*, 4–11.

Timbal, B., et al. (2010), Understanding the anthropogenic nature of the observed rainfall decline across south-eastern Australia, *CAWCR Tech. Rep. 26*, Cent. for Aust. Weather and Clim. Res., Melbourne, Victoria.

Ummenhofer, C. C., M. H. England, P. C. McIntosh, G. A. Meyers, M. J. Pook, J. S. Risbey, A. Sen Gupta, and A. S. Taschetto (2009), What causes southeast Australia's worst droughts?, *Geophys. Res. Lett.*, *36*, L04706, doi:10.1029/2008GL036801.

Vaze, J., F. H. S. Chiew, J.-M. Perraud, N. Viney, D. Post, J. Teng, B. Wang, J. Lerat, and M. Goswami (2010), Rainfall-runoff modelling across southeast Australia: Datasets, models and results, *Aust. J. Water Resour.*, *14*, 101–116.

Verdon-Kidd, D. C., and A. S. Kiem (2009), Nature and causes of protracted droughts in southeast Australia: Comparison between the Federation, WWII, and Big Dry droughts, *Geophys. Res. Lett.*, *36*, L22707, doi:10.1029/2009GL041067.

Vogel, R. M., I. Wilson, and C. Daly (1999), Regional regression models of annual streamflow for the United States, *J. Irrig. Drain. Eng.*, *125*, 148–157.

Yu, J., G. Fu, W. Cai, and T. Cowan (2010), Impacts of precipitation and temperature changes on annual streamflow in the Murray-Darling Basin, *Water Int.*, *35*, 313–323, doi:10.1080/02508060.2010.484907.

Zhang, L., W. R. Dawes, and G. R. Walker (2001), Response of mean annual evapotranspiration to vegetation changes at catchment scale, *Water Resour. Res.*, *37*, 701–708, doi:10.1029/2000WR900325.

F. H. S. Chiew and N. J. Potter, CSIRO Water for a Healthy Country National Research Flagship, CSIRO Land and Water, GPO Box 1666, Canberra, ACT 2601, Australia. (nick.potter@csiro.au)